A LETTERS JOURNAL EXPLORING THE FRONTIERS OF PHYSICS

OFFPRINT

Evolution of granular packings by nonlinear acoustic waves

S. VAN DEN WILDENBERG, M. VAN HECKE and X. JIA

EPL, **101** (2013) 14004

A Letters Journal Exploring the Frontiers of Physics

January 2013

EPL, **101** (2013) 14004
doi: 10.1209/0295-5075/101/14004

www.epljournal.org

Evolution of granular packings by nonlinear acoustic waves

S. van den Wildenberg[1,2], M. van Hecke[2] and X. Jia[1,3]

[1] *Université Paris-Est, Laboratoire de Physique des Matériaux Divisés et des Interfaces 77454 Marne La Vallée, France, EU*
[2] *Kamerlingh Onnes Laboratorium, Universiteit Leiden - P.O. Box 9504, 2300 RA Leiden, The Netherlands, EU*
[3] *Institut Langevin, ESPCI ParisTech, CNRS UMR 7587 - 1 rue Jussieu, 75005 Paris, France, EU*

received 24 September 2012; accepted in final form 2 January 2013
published online 22 January 2013

PACS 45.70.-n – Granular systems
PACS 43.35.+d – Ultrasonics, quantum acoustics, and physical effects of sound
PACS 91.30.-f – Seismology

Abstract – We investigate the nonlinear response of pulsed high-amplitude sound transmission in weakly compressed granular materials, simultaneously probing sound amplitude, time-of-flight velocity and harmonic generation. We observe that weakly compressed packings can both exhibit weakening and strengthening when driven by high-amplitude sound, and that weakening/strengthening of the sound velocity and transmission amplitude go hand in hand. We find that strengthening is associated with the generation of second harmonics, whereas for weakening, no appreciable second harmonics are generated. All these findings point to changes in the contact network; effective medium theory can describe these effects qualitatively, but fails to account for them quantitatively.

Dry granular media are collections of macroscopic grains that interact through repulsive and frictional contact forces, and that jam in nonequilibrium configurations [1–4]. The root cause of their rich behavior is that for given values of macroscopic control parameters, such as density and pressure, there are many microstates, which are not equivalent [5–8]. Perhaps the most crucial characteristics of these microstates are their highly heterogenous contact force networks that can quickly rearrange under driving [5]. A particularly important quantity that characterizes these networks is the contact number Z, defined as the average number of contacts per particle. This contact number plays a central role in the mechanical behavior of a granular system [2–4,9,10], but is hard to observe directly in 3D, when using standard techniques such as photoelastic imaging [5], X-ray tomography, MRI and fluorescent confocal microscopy [11,12].

Sound waves propagate through the contacts between grains, making sound an alternative and unique probe to examine 3D contact networks [13,14]. For long-wavelength, low-amplitude waves propagating in granular media, effective medium theory (EMT) might be applicable [14]. In such theories, one assumes that spatial fluctuations of contact density and contact stiffness can be ignored —reasonable for long wavelengths. Consequently, measurements of the compressional and shear wave velocities, V_P and V_S, give access to the contact number Z, via $V_P \propto (Z/R\rho)^{1/2}(D_n + 2D_t/3)^{1/2}$ and $V_S \propto (Z/R\rho)^{1/2}(D_n + 3D_t/2)^{1/2}$, where R is the elastic-sphere radius, ρ the material density of spheres and D_n and D_t are the normal and tangential contact stiffness, respectively [14]. For Hertzian contacts, the Hertz-Mindlin contact theory predicts that $D_n(P)$ and $D_t(P)$ are proportional to $P^{1/3}$, which yields the well-known pressure dependence of V_P and V_S as $Z^{1/3}\phi^{-1/6}P^{1/6}$, with ϕ the packing density.

Whereas some properties of granular media, such as low-amplitude sound velocity or bulk elastic moduli, are well captured by effective medium theory [13,14], other properties, such as their nonlinear response to high-amplitude pulsed sound waves [15] or weak shaking [7] evidence their rich, glassy behaviour. Underlying this richness is the fragility of granular media. Indeed, for typical grain sizes (600–800 μm) and confining pressures (say 1–100 kPa), the elastic deformations (6–120 nm) of rigid grains such as glass beads are orders of magnitude smaller than the grain size. Hence, even tiny deformations may be sufficient to change contact forces and open and close contacts [16]. As a result, when granular systems are driven by external forces, subtle changes in the microscopic organization

of the grains can lead to significant changes in their bulk properties, without any appreciable change in macroscopic parameters such as density.

In this nonlinear regime, Liu and Nagel showed that the transmitted sound amplitudes of high-amplitude continuous waves traveling through a glass bead packing under gravity exhibit strong temporal fluctuations [8]. This evolution is likely associated with vibration-induced changes in the microscopic fabric, such as the breaking and reforming of particle contacts. Similarly fluctuating behavior has also been found for the phase velocity of sound waves [17]. In addition, in several cases, the effective sound velocity in granular media was found to decrease under the influence of strong sound waves. This weakening is likely due to the decrease of the tangential stiffness D_t, and/or the loss of contacts by acoustically induced sliding of grains which results in the rearrangement of the contact network [15,18].

These observations raise several interesting questions. Is there any correlation between amplitude and velocity measurements of the nonlinear sound transmission? Why does nonlinear sound lead to weakening, not strengthening of granular media? Can we elucidate the microscopic behavior governing acoustically induced granular evolution?

In this work, we address these questions by investigating long-wavelength pulsed compressional waves in weakly compressed granular media. We present the first simultaneous measurements of sound amplitude, time-of-flight velocity and harmonic generation. Our first finding is that weakly compressed packings can both exhibit weakening and strengthening, and that weakening/strengthening of the sound velocity and the amplitude of the transmitted signal go hand in hand. Our second main finding is that strengthening is associated with the generation of second harmonics, whereas for weakening, no second harmonics are generated. We suggest that this strong correlation can be interpreted via sound-induced buckling and sliding that, respectively, raise and diminish the contact number.

Experimental procedure. – Our acoustic measurements were performed on a granular medium consisting of polydisperse glass beads (600–800 μm), in which a first broadband piezoelectric transducer of diameter 30 mm was used as acoustic source, while a second transducer placed at a distance of 9 cm from the source detects the propagation of coherent longitudinal waves (fig. 1(a)).

Two types of mechanical loading were applied in this work. In the first set of experiments, we used a cylindrical container of diameter 150 mm and height 200 mm. A pre-compaction of the granular packing is realized by 20 cycles of loading-unloading of a top piston, up to a pressure of about 110 kPa. In this way, a reproducible packing was obtained and acoustic measurements were then performed at a pressure $P = 40$ kPa. The second set of experiments was carried out in a setup consisting of the same glass beads confined in a square Plexiglas box

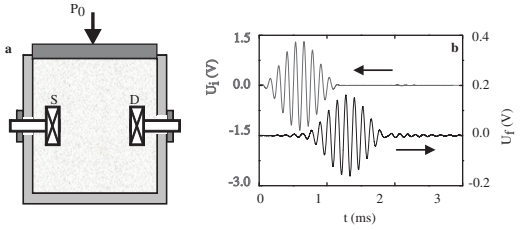

Fig. 1: (a) Schematic of the experimental setup where glass beads are confined by a vertical stress of $P = 40$ kPa. Compressional waves are excited by a source transducer S and detected by a second transducer D. (b) A typical input wave U_i consisting of a ten-cycle Gaussian tone burst centered at $f = 9$ kHz (top, grey) and the transmitted wave U_f (bottom, black).

(325 mm × 300 mm × 150 mm) with a free top surface [19]. The source and detector where burried at a depth of 11 cm, leading to an effective pressure of about $P = 2$ kPa. Before each experiment, the granular sample was freshly poured, and the container was horizontally shaken to obtain a stable packing.

We send ten-cycle Gaussian tone bursts centered at a low frequency (in the 8–10 kHz range) every 50 ms. The obtained data averaged over ~ 1 s allows us to simultaneously measure the sound velocity V and the magnitude and harmonic content of the transmitted signal. The sound velocity was determined from the time-of-flight velocity V between the excitation and the transmitted Gaussian pulses (fig. 1(b)) —no appreciable dispersion of the sound velocity was observed in the frequency range 1–100 kHz. We note here that typical wavelengths are of order 1 cm, smaller than the detector, but significantly larger than the beads, so that our sound waves probe the granular medium at an intermediate scale.

We characterize the transmitted signal by the amplitude of the fundamental component and the second harmonic. To do so, we filter the detected waves in the time domain using custom written Labview routines, and determine the amplitudes U_f of the fundamental and U_{2f} of the second harmonic by fitting Gaussian profiles to the appropriately filtered signal [18]. This allows us to probe the evolution of V, U_f and U_{2f} as a function of the input amplitude U_i and time t.

Strengthening and weakening of compressed samples. – We probe the evolution of the granular medium under the influence of nonlinear sound by measuring both the amplitude and time-of-flight velocity of the transmitted acoustic signal as a function of time. We first focus on our well-compressed sample ($P = 40$ kPa), using ten-cycle pulses centered at 8 kHz and fixing $U_i = 90$ mV, corresponding to a vibration displacement of about 10 nm (acceleration 2–3 g).

As figs. 2(a), (b) illustrate, both the velocity V and the ratio U_f/U_i show a significant time evolution, even as the input strength is kept constant: the granular packing is modified by the sound waves [8]. We stress that the evolu-

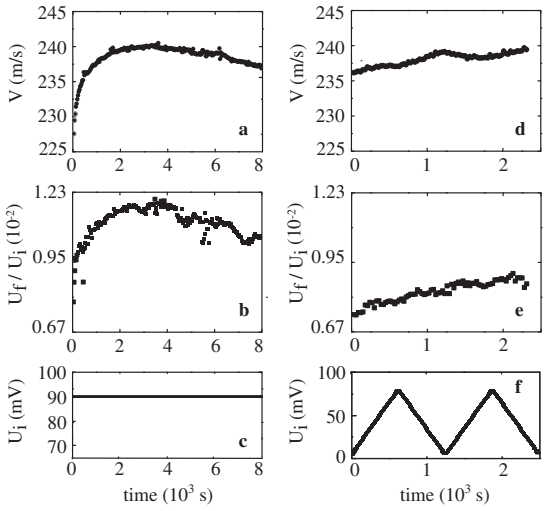

Fig. 2: Interaction of high-amplitude sound waves with a bead packing under $P = 40$ kPa. (a)–(c) Constant input; (d)–(f) sweeps. (a), (d): evolution of sound velocity V. (b), (e): evolution of the ratio of transmitted first harmonic, U_f, and input U_i. (c), (f): U_i.

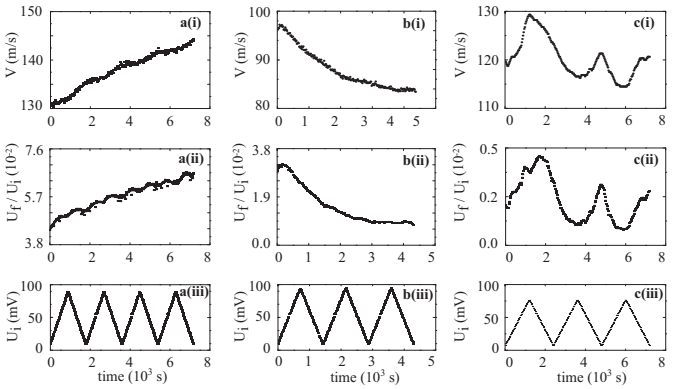

Fig. 3: Typical measurements of the sound velocity (i) and the amplitude ratio (ii) measured as a function of time in a loose granular packing under $P = 2$ kPa, excited by a given protocol (iii). Three distinct regimes are observed: (a) strengthening, (b) weakening, and (c) interplay between strengthening and weakening.

tion of the amplitude ratio and the sound velocity appear very similar. Surprisingly, this evolution is not always monotonic: In the experiments shown in figs. 2(a),(b), both amplitude and velocity of the transmitted wave increase from 0 to 3000 s, corresponding to a strengthening of the granular packing, whereas from 3000 to 8000 s, the amplitude and the velocity decreased, implying a weakening of the granular packing [15].

During the experiment, we do not observed any visible rearrangement of the grains or measure any significant change in the height of the granular sample. We estimate the maximal change in the height to be less than 10 μm, corresponding to a change in packing fraction less than 0.1%. This is significantly less from density changes seen in tapping experiments [6], and far too small to explain by itself the observed evolution of our packings.

To probe the role of the excitation amplitude, we performed similar acoustic measurements by ramping the input amplitude U_i up and down. As figs. 2(d)–(f) illustrate, the strengthening or weakening does not simply correlate to an increase or decrease of the excitation amplitude as would be expected for solitonic or shock waves [20,21] the observed changes in transmission and sounds speed are not simply due to such nonlinear effects, but rather suggest an evolution of the packing.

Repeating these experiments, both with fixed and varying U_i, and for different sweep rates, we did not find a clear correlation between the excitation protocol and the strengthening or weakening behavior, although we note that immediately after loading the initial behavior is always strengthening.

Strengthening and weakening of weakly compressed samples. – The time evolution of our granular samples must be caused by microscopic changes in the contact fabric, which we expect to be more easily excited at lower pressures. We conducted a second series of experiments in a packing of glass beads under gravity, and focus on the protocol where U_i is ramped up and down. We undertook a total of 21 runs.

As fig. 3 illustrates, we observe three distinct types of behavior: strengthening (fig. 3(a), 9 times), weakening (fig. 3(b), 8 times), or, more rarely, random variation between strengthening and weakening (fig. 3(c), 4 times). The random nature of the weakening or strengthening confirms that the type of evolution is not only controlled by the sound amplitude, but also depends on the history and particular microstate of the granular packing itself. We note that the sound velocity variation observed at this low pressure is about 10%, larger than the 4% observed at higher pressures ($P = 40$ kPa), consistent with our expectation that lower pressures promote the evolution of the packing.

The striking similarity that we observed between the temporal variations in the amplitude ratio and in the sound velocity can be qualitatively understood in terms of the acoustic impedance using an effective medium approach, as follows: The acoustic impedance of the granular material is $z_g := \rho V$, where ρ and V are the mediums density and the effective sound velocity, and the transducers have a much higher impedance z_t. The coefficient of amplitude transmission for a plane wave from the source transducer to the granular medium is given by $t_1 = 2z_t/(z_t + z_g)$, whereas the transmission coefficient from the granular medium to the detection transducer $t_2 = 2z_g/(z_t + z_g)$, so that the coefficient of the total transmission t is thus

$$t = t_1 t_2 = 4 z_g z_t / (z_g + z_t)^2 \approx 4 z_g / z_t \propto \rho V. \qquad (1)$$

Since we did not measure a significant change in the height of the granular sample, we argue that the packing density

ρ remains almost constant, so that it follows that in this framework, the amplitude of sound transmission should be linearly proportional to the sound velocity.

While this is qualitatively consistent with our observations, we note here that the variation in amplitude is much stronger than the variation in sound velocity —for example, in fig. 3(b), the change in V is of order 15%, whereas the change in U_f/U_i is more than a factor 2! Comparing the changes in V and U_f/U_i of all our data, we conclude that the typical change in transmission amplitude is roughly five times larger than the change in velocity. This suggest that effective medium theory can not quantitatively account for the evolution of the packing by nonlinear sound waves: the physics underlying the evolution of the packing is truly complex.

Harmonic generation. – On the scale of the grain contacts, two types of nonlinearity can be distinguished [22]: one arises from the normal loading (Hertzian model) and the other from the tangential friction force (Mindlin model). It is useful to distinguish a weakly and strongly nonlinear regime, by the relative magnitude of the sound amplitude u and the typical static grain deformation u_0, induced by the confining pressure. The highly nonlinear regime corresponds to $u \gg u_0$, shock waves can be generated with a front velocity depending on the wave amplitude, strongly damped by plastic rearrangement and frictional dissipation [17,20,21,23]. On the other hand, in the weakly nonlinear regime ($u \ll u_0$), reversible nonlinear responses described by the nonlinear terms of the normal stiffness [24] have been observed, including second-harmonic generation [18].

To gain more insight into the microscopics underlying the strengthening and weakening, we have probed the magnitude of the second harmonic. As we will detail below, the Hertzian nonlinearity in the normal forces, associated with changes in the particles overlap, will give rise to second-harmonic generation, with a magnitude U_{2f} that is expected to rise as U_i^2. In contrast, nonlinearities due to sliding or transversal motion of contacting grains, described by the full Hertz-Mindlin interactions, do not generate second harmonics, due to symmetry ("sliding left is equivalent to sliding right"). Our central finding is a one-to-one correlation between strengthening and the generation of second harmonics on the one hand, and weakening and the absence of second harmonics, on the other hand.

To correlate strengthening/weakening and second-harmonic generation, we focus on all 17 data sets taken at 2 kPa that monotonically weaken or strengthen. As figs. 4(a), (b) illustrate, we first will study scatter plots of U_{2f} *vs.* U_i.

Let us first focus on fig. 4(a) which shows harmonic generation for a strengthening sample (the same as depicted in fig. 3(a). Here, the second-harmonic U_{2f} grows quadratically with U_i. We show now that this is consistent with the Hertzian nonlinearity of the normal

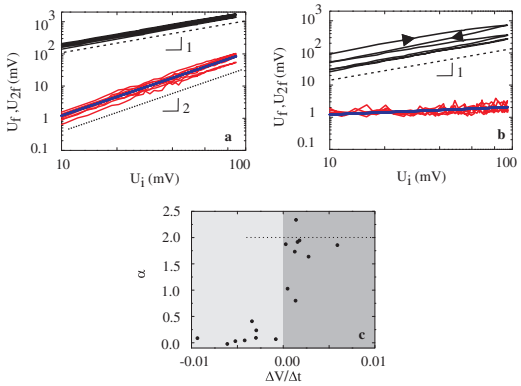

Fig. 4: (Color online) Second-harmonic generation measured in the packings of fig. 3. (a) The fundamental U_f (black circles) and second harmonic U_{2f} (red crosses) measured *vs.* U_i during strengthening. Linear and quadratic scaling (dashed and dotted lines) are shown as a guide to the eye. (b) U_f (black circles) and second harmonic U_{2f} (red crosses) measured *vs.* U_i during weakening. The straight blue line corresponds to the best fit. (c) Scatter plot of power law exponent α *vs.* $\Delta V/\Delta t$ for U_{2f} shows that $\alpha \approx 2$ for strengthening samples (dark-grey shade), whereas $\alpha \approx 0$ for weakening samples (light-grey shade). Error bars on α are or order 20%.

forces between grains, where the contact force F between two particles scales as $\delta^{3/2}$, where δ is the particles deformation. Here, δ is composed of two contributions: a constant δ_0, which in a mean-field approximation is set by the pressure, and an oscillation contribution u_n, which is due to the sound wave. Expanding the Hertzian contact law around $\delta = \delta_0$, we find that the oscillating component of the force between particles $F_n \approx D_n u_n(1 + \beta u_n + \delta u_n^2 + \ldots)$, where D_n is the linear normal stiffness, and β and δ correspond to the quadratic and cubic nonlinear terms determined by the confining pressure P [15]. From this, we can obtain an approximate expression for the second-harmonic displacement within effective medium approaches $U_{2f} \propto \beta f^2 U_i^2$ [18], which is precisely the power law observed in fig. 4(a).

Let us now turn to fig. 4(b), which shows the absence of significant second-harmonic generation in a weakening sample. Clearly, the magnitude of the normal relative motion u_n is too small to excite a significant second harmonic, but nevertheless, the amplitude of the sound wave is similar — what is going on? We suggest that in this case, the relative motion between particles is mainly in the perpendicular, sliding direction. We may deduce from the Mindlin theory an approximate relation between the shear oscillating displacement u_t and force F_t, $u_t \approx S_t F_t + \gamma F_t^3 + \ldots$, where S_t is the nonlinear dynamic compliance [15] and γ the cubic nonlinear term. The absence of a quadratic nonlinear term is due to symmetry, which implies that nonlinear effects like harmonics generation are one order smaller than for the normal oscillation [25], and would explain the absence of an appreciable second harmonic in the weakening regime shown in fig. 4(b).

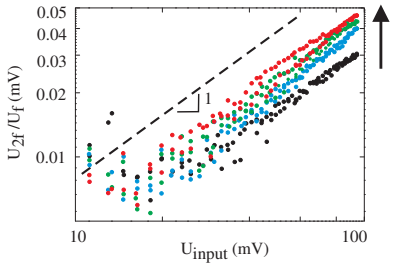

Fig. 5: (Color online) Amplitude ratio between the second harmonic and fundamental component of fig. 4(a), obtained during the sequential excitation cycles: 1st cycle up-down (black), 2nd cycle up-down (blue), 3rd cycle up-down (green) and 4th cycle up-down (red). The second-harmonic generation increases with the number of cycles, as indicated by the arrow.

The generality of the link between strengthening/weakening and second-harmonic generation is illustrated in fig. 4(c). Here we have characterized all data sets (not just those shown in figs. 4(a) and (b)) by the overall time evolution of the sound velocity, $\Delta V/\Delta t$, and an exponent α, obtained by fitting a power law expression of the form $U_{2f} = AU_i^{\alpha}$ to the scatter plots of U_{2f} *vs.* U_i. fig. 4(c) shows the resulting scatter plot of the exponent α as a function of $\Delta V/\Delta t$. Clearly, the exponent goes from a value around zero (for $\Delta V/\Delta t < 0$) to a value around two (for $\Delta V/\Delta t > 0$). Even though the drift in sound velocity is not linear, this shows that $\Delta V/\Delta t$ captures the sign of this drift, *i.e.*, strengthening *vs.* weakening.

Figure 4(c) thus illustrates the generality of our finding that for strengthening samples, the second harmonic U_{2f} grows quadratically with U_i, consistent with a simple Hertzian nonlinearity, whereas for weakening samples, U_{2f} is small and nearly independent of U_i, suggesting that in the weakening regime the Hertzian nonlinearity is not dominant and likely overshadowed by the frictional nonlinearity [15].

Finally, we have revisited the limited number of runs that show alternating strengthening and weakening, and have inspected the magnitude of the second harmonic. We note that when a sample switches from strengthening to weakening, the second harmonic does not drop immediately, suggesting that the harmonic generation follows, and not precedes, the strengthening or weakening of the sample.

Evolution of harmonics. – During strengthening, the packing continues to evolve over several sweeps of U_i. As shown in fig. 5, the second harmonic U_{2f} also keeps growing in strength. This growth is *not* only simply due to U_i becoming larger — by plotting the ratio of U_{2f}/U_f as a function of U_i, we find that also this ratio increases over time, indicating that the generation of the second harmonics becomes more efficient as the sample strengthens. Again, this evidences the complexity of the evolution of the granular packing.

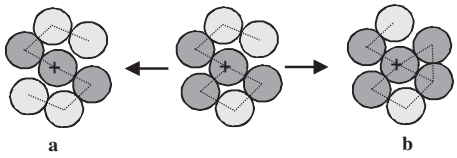

Fig. 6: Schematic illustrations of sound-induced change in the mechanical coordination number: (a) a decrease via acoustic fluidization; (b) an increase via buckling. The associated packing density and geometric coordination number remain unchanged in all these cases.

Discussion and conclusion. – Our data of the transmission of nonlinear sound pulses in weakly compressed granular packings reveals strong evolution of the velocity and amplitude of these pulses as well as its harmonic generation. A simple effective medium picture captures the correlation between weakening/strengthening of sound velocity and transmission amplitude qualitatively, but fails to quantitatively capture the magnitude of these effects. Similarly, the generation of second harmonics in the strengthening regime is consistent with the Hertzian nonlinearity of the normal force components, but this nonlinearity itself is not sufficient to capture the magnitude of strengthening/weakening [15].

We suggest that changes in the contact number Z are an essential step towards understanding the magnitude of the observed strengthening and weakening phenomena. Based on the coincidence of an increase of sound velocity and transmission amplitude with second-harmonic generation, we conjecture the following picture (see fig. 6). In the weakening regime, the tangential vibration between jammed particles reduces the contact stiffness D_t via the frictional nonlinearity and further causes the loss of contacts via sliding of particles out of contact $\Delta Z < 0$ (fig. 6(a)), a process previously refereed to as acoustic fluidization [15]. Since the frictional nonlinearity does not generate even harmonics, this is consistent with the observed absence of second harmonics in the weakening regime (fig. 4).

In contrast, in the strengthening regime, large normal vibrations take place (as evidenced by the observed generation of second harmonics), and these vibrations lead to buckling of the force chains —a dynamic counterpart of pressure-induced particle buckling [26]. This mechanism would result in the formation of new contacts involved in the force chains $\Delta Z > 0$ (fig. 6(b)), driving the system to a mechanically more stable configuration. Note that this mechanism is different from the particle buckling mechanism induced by compression, which is accompanied with a packing fraction change [26–28].

While in frictional packings, changes in the overall contact number Z may arise without appreciable changes of the packing fraction, we believe that such contact changes, although important, only capture part of the physics: First, according to effective medium theory [14], the measured variation of the sound velocity $\Delta V/V \sim 10\%$

(fig. 3) would correspond to $\Delta Z/Z \approx 3\Delta V/V \sim 30\%$, close to a relative variation between random close packing ($Z_{RCP} \approx 6$) and random loose packing ($Z_{RLP} \approx 4$) [2–4, 9,10]. It is unlikely that such large changes in the contact number can arise without appreciable changes in the packing fraction. Second, changes in the contact number alone do not capture the discrepancy between the typical variation in the sound velocity and the transmission amplitude —recall that the change in the latter is typically five times larger than the change in the former. Both of these observations illustrate that the effective medium theory qualitatively describes the experiments, but fails to quantitatively account for the data. We suggest that the changes in contact numbers lead to significant rearrangements of the contact network, which eventually result in the breakdown of the affine approximations underlying EMT.

Our experiments therefore evidence evolution of the packing beyond what can be captured by effective medium theories. Important questions raised by this work then include, first, what causes the system to collectively strengthen or weaken and, second, what models can quantitatively capture the large variation in sound velocity and sound transmission observed.

* * *

We would like to thank J. Laurent for assistance to the under-gravity experiment and H. Sizun for the cell realization. SvdW acknowledges funding from Shell and the research programme of the Foundation for Fundamental Research on Matter (FOM), which is part of the Netherlands Organisation for Scientific Research (NWO). MvH acknowledges support from NWO/VICI.

REFERENCES

[1] Liu A. and Nagel S., *Nature*, **396** (1998) 21.
[2] Song C., Wang P. and Makse H. A., *Nature*, **453** (2008) 629.
[3] van Hecke M., *J. Phys.: Condens. Matter*, **22** (2010) 033101; Somfai E., van Hecke M., Ellenbroek W. G., Shundyak K. and van Saarloos W., *Phys. Rev. E*, **75** (2007) 020301.
[4] Wyart M., Nagel S. R. and Witten T. A., *Europhys. Lett.*, **72** (2005) 486; O'Hern C. S., Silbert L. E., Liu A. J. and Nagel S. R., *Phys. Rev. E*, **68** (2003) 011306.
[5] Jaeger H. M., Nagel S. R. and Behringer R. P., *Rev. Mod. Phys.*, **68** (1996) 1259.
[6] Nowak E. R., Knight J. B., Ben-Naim E., Jaeger H. M. and Nagel S. R., *Phys. Rev. E*, **57** (1998) 1971.
[7] Umbanhowar P. and van Hecke M, *Phys. Rev. E*, **72** (2005) 030301.
[8] Liu C. H. and Nagel S. R., *Phys. Rev. Lett.*, **68** (1992) 2301.
[9] Agnolin I. and Roux J.-N., *Phys. Rev. E*, **76** (2007) 061304.
[10] Zhang L. and Thornton C., *Géotechnique*, **57** (2007) 343; Cui L. and O'Sullivan C., *Géotechnique*, **56** (2006) 455.
[11] Mueth D. M. *et al.*, *Nature*, **406** (2000) 385.
[12] Brujic J. *et al.*, *Faraday Discuss.*, **123** (2003) 207.
[13] Jia X., Caroli C. and Velicky B., *Phys. Rev. Lett.*, **82** (1999) 863.
[14] Makse H. A., Gland N., Johnson D. L. and Schwartz L., *Phys. Rev. E*, **70** (2004) 061302; Winkler K. W., *Geophys. Res. Lett.*, **10** (1983) 1073; Walton K., *J. Mech. Phys. Solids*, **35** (1987) 213.
[15] Jia X., Brunet T. and Laurent J., *Phys. Rev. E*, **84** (2011) 020301(R).
[16] Owens E. T. and Daniels K., *EPL*, **94** (2011) 54005; Schreck C. F., Bertrand T., OHern C. S. and Shattuck M. D., *Phys. Rev. Lett.*, **107** (2011) 078301.
[17] Hostler S. R. and Brenne C. E., *Phys. Rev. E*, **72** (2005) 031303.
[18] Brunet T., Jia X. and Johnson P., *Geophys. Res. Lett.*, **35** (2008) L19308.
[19] Laurent J., PhD Thesis, Université Paris-Est Marne-la-Vallée, July 2011, in French.
[20] Nesterenko V. F., *Dynamics of Heterogeneous Materials* (Springer, New York) 2001; Daraio C. *et al.*, *Phys. Rev. Lett.*, **96** (2006) 058002; Sen S. *et al.*, *Phys. Rep.*, **462** (2008) 21; Huillard G., Noblin X. and Rajchenbach J., *Phys. Rev. E*, **75** (2011) 021304; Gomez L., Turner A., van Hecke M. and Vitelli V., *Phys. Rev. Lett.*, **108** (2012) 058001.
[21] van den Wildenberg S., van Loo R. and van Hecke M., in preparation.
[22] Johnson K. L., *Contact Mechanics* (Cambridge University Press, Cambridge) 1985.
[23] Brunet T., Jia X. and Mills P., *Phys. Rev. Lett*, **101** (2008) 138001.
[24] Ostrovsky L. A. and Johnson P. A., *Riv. Nuovo Cimento*, **24**, issue No. 7 (2001) 1; Tournat V., Zaitsev V., Nazarov V., Gusev V. and Castagnde B., *Acoust. Phys.*, **51** (2005) 543.
[25] Catheline S., Gennisson J.-L., Tanter M. and Fink M., *Phys. Rev. Lett.*, **91** (2003) 164301.
[26] Goddard J. D., *Proc. R. Soc. London, Ser. A*, **430** (1990) 105.
[27] Roux J.-N., in *Powders and Grains 1997* (Balkema, Rotterdam) 1997, pp. 215–218; Jia X. and Mills P., in *Powders and Grains 2001* (Balkema, Lisse) 2001, pp. 105–112.
[28] Pilbieam C. A. and Vaisnys J. R., *J. Geophys. Res.*, **78** (1973) 810.